Dynamical quark mass and finite volume effects in the Dyson-Schwinger equations*

Li-Juan Zhou (周丽娟)[1,2†] De-Xian Wei (韦德贤)[2] Zhong-Yi Liu (刘中一)[3] Hong-Wei Zhong (钟红伟)[2]

[1]Liuzhou Polytechnic University, Liuzhou 545006, China
[2]School of Science, Guangxi University of Science and Technology, Liuzhou 545006, China
[3]School of Mathematical Sciences and Statistics, Baise University, Baise 533000, China

Abstract: Within the framework of Dyson-Schwinger equations (DSEs) and by means of the Multiple Reflection Expansion approximation, we study the finite volume effects on the constituent quark mass in a strong external magnetic field. Since the magnetic field influences the coupling constant, which controls the strength of strong interactions in QCD, we adopt the magnetic-field-dependent running coupling constant in our simulations. The results show that, in addition to the magnetic field, the masses of constituent quarks also have a significant dependence on the volume and the running coupling constant. The model behaves closely to the infinite volume limit for large sizes, but the effect of the finite volume is significant when the system size R is about $2-6$ fm. The finite volume effects and the magnetic-field-dependent running coupling constant have considerable influence on the phase transition.

Keywords: Dyson-Schwinger equations, magnetization phenomena, phase transition, multiple reflection expansion, running coupling constant

DOI: 10.1088/1674-1137/ae4583 **CSTR:** 32044.14.ChinesePhysicsC.50053106

I. INTRODUCTION

Studying the QCD phase transition is always challenging in high-energy physics since the research may reveal the nature of the early universe matter evolution [1−3]. The transitions include the chiral phase transition and the confinement transition. Many physical parameters affect the QCD phase transition. Besides the temperature and chemical potential, magnetic field and system volume also affect the transition. The system generated in heavy-ion collision experiments has a finite volume that depends on the size of the colliding nuclei, the collision center of mass energy, and the centrality of collision [4−6]. In Refs. [7−9], it was estimated that the quark-gluon plasma (QGP) system produced at the relativistic heavy ion collision (RHIC) could have sizes between 2 fm and 10 fm. So, an understanding of finite volume effects is very important for the relativistic heavy ion collision.

Theoretical physicists have proposed many theoretical models to study the finite volume effects on strongly interacting systems, including the Nambu-Jona-Lasinio (NJL) model [10, 11], the quark-meson model [12, 13], the non-interaction bag model [14], and Dyson-Schwinger Equations (DSEs) [15−21]. For the sake of convenience, most of these studies consider the systems as a cube, using antiperiodic boundary conditions (APBC) as well as periodic boundary conditions (PBC). However, if the volume of the fireball is small, we must take the system size and shape into account. This leads us to consider a more realistic approach to study the QCD phase transition. In this work, we adopt the Multiple Reflection Expansion (MRE) approximation [22−25], which considers the surface and curvature contributions.

With the development of experiments, very strong magnetic fields have been generated in noncentral heavy-ion collision experiments. Since quarks are electrically charged and can be coupled to the magnetic field, the magnetic field has a great influence on the QCD phase transition. A natural question that emerges is what is the effect of the magnetic field produced in collisions on the QCD phase transition in a finite volume system. This question has been partially studied in Refs. [26−28]. In addition, it has been confirmed that the magnetic field

Received 20 August 2025; Accepted 11 February 2026; Accepted manuscript online 12 February 2026

* Li-Juan Zhou has been supported by the National Natural Science Foundation of China (11865005), the Natural Science Foundation of Guangxi (China) (2025GXNSFAA069552). De-Xian Wei has been supported by the National Natural Science Foundation of China (12105057), the Natural Science Foundation of Guangxi (China) (2023GXNSFAA026020)

† E-mail: zhoulj@gxust.edu.cn

also exerts an influence on the coupling constant [29]. Researchers have worked hard to construct a magnetic-field-dependent running coupling constant [30−33]. In the presence of a magnetic field, we believe constructing a more realistic framework that aligns with the physical coupling strength of QCD is reasonable and necessary. Nevertheless, the incorporation of QCD properties and the substantial computational challenges associated with solving the coupled equations remain significant hurdles.

In our previous works, we have studied the condensate and magnetization phenomena in strong external magnetic fields using the DSEs. The results showed that such condensate and magnetization phenomena are dependent on the magnitude of the magnetic field [34, 35]. As we know, the system created in RHIC exists in a finite size rather than a thermodynamical limit. To determine the freeze-out parameters in experiments, one has to take the finite size and the running coupling constant into account. Therefore, in this paper, we adopt a different approach based on the DSEs, utilizing the MRE formalism to investigate the finite volume effects of strongly interacting matter with a magnetic-field-dependent running coupling constant. We study its influence on the quark condensate and the constituent quark mass. Compared to other methods, it is more natural to study the QGP fireball by means of MRE, which describes a sphere rather than a cube.

The paper is organized as follows: In Sec. II, we give a brief introduction to the DSEs, the MRE formalism, and the magnetic-field-dependent running coupling constant. By solving the DSEs in finite volume with the magnetic-field-dependent running coupling constant, we show the numerical results in Sec. III. Finally, we summarize the main results in Sec. IV.

II. THEORY MODEL

A. Dyson-Schwinger equations

In this section, we will briefly review the formulation of DSEs. We start with the quark propagator. The DSEs in position space with a local interaction are given by

$$S^{-1}(x,y) = S_0^{-1}(x,y) + \Sigma(x,y), \tag{1}$$

where S^{-1} is the inverse of the dressed quark propagator, S_0^{-1} is the inverse of the free quark propagator, and the quark self-energy is given by

$$\Sigma(x,y) = \mathrm{i}g^2 C_F \gamma^\mu S(x,y)\Gamma^\nu(y) D_{\mu\nu}(x,y), \tag{2}$$

with g as the coupling constant of strong interaction, $C_F = (N_c^2-1)/N_c$, Γ^ν as the dressed quark-gluon vertex, and $D_{\mu\nu}$ denoting the gluon propagator in the Landau gauge. We expand Eq. (1) in terms of Ritus transformation functions, multiplying this equation by $\bar{E}_p(x)$ from the left and $E_{p'}(y)$ from the right, which serves as a substitute for the usual Fourier exponential factor $e^{ip\cdot x}$. The integration over x and y yields

$$\begin{aligned}&\int \mathrm{d}^4x\mathrm{d}^4y \bar{E}_p(x) S^{-1}(x,y) E_{p'}(y)\\ =&\int \mathrm{d}^4x\mathrm{d}^4y \bar{E}_p(x) S_0^{-1}(x,y) E_{p'}(y)\\ &+\int \mathrm{d}^4x\mathrm{d}^4y \bar{E}_p(x)\Sigma(x,y) E_{p'}(y).\end{aligned} \tag{3}$$

Using

$$\begin{aligned}&\int \mathrm{d}^4x \bar{E}_p(x) E_{p'}(x) = (2\pi)^4\delta^4(p-p')\Pi(L),\\ &\sum_{L=0}^{\infty}\int \frac{\mathrm{d}^2p_\parallel}{(2\pi)^4}\int_{-\infty}^{\infty}\mathrm{d}p_2 E_p(x)\bar{E}_p(y) = (2\pi)^4\delta^4(x-y),\end{aligned} \tag{4}$$

and

$$\Pi(L) = \begin{cases}\Delta(\mathrm{sgn}(eB)), & L=0,\\ 1, & L>0,\end{cases} \tag{5}$$

one obtains

$$\begin{aligned}&(2\pi)^4\delta^4(p-p')\Pi(L)\left[A_0(p) + A_\parallel(p)\mathrm{i}\gamma\cdot p_\parallel + A_\perp(p)\mathrm{i}\gamma\cdot p_\perp\right]\\ &= (2\pi)^4\delta^4(p-p')\Pi(L)\left[\gamma p + m\right] + \Sigma(p,p'),\end{aligned} \tag{6}$$

where A_0, $A_\parallel$, and $A_\perp$ are the scalar and vector quark dressing functions of the quark propagator in (pseudo-)momentum space, and $\Sigma(p,p')$ denotes the self-energy. The momentum vectors parallel and perpendicular to the magnetic field direction are denoted by $p_\parallel = (p_0, 0, 0, p_3)^T$ and $p_\perp = (0, 0, p_2 = \sqrt{2|eB|L}, 0)^T$, where eB is the magnitude of the magnetic field, and L is the total angular momentum quantum number for each Landau level. The self-energy term is implicitly proportional to $\delta^4(p-p')\Pi(L)$. The quark self-energy in the Ritus eigenbasis is then given by

$$\Sigma(p,p') = g^2 C_F \int \mathrm{d}^4x\mathrm{d}^4y \bar{E}_p(x)\gamma^\mu S(x,y)\Gamma^\nu(y) D_{\mu\nu}(x,y) E_{p'}(y), \tag{7}$$

where $S(x,y)$ is the fermion propagator. The representation of the fermion propagator in Ritus's representation is given by

$$S(x,y)=\sum_{L=0}^{\infty}\int\frac{\mathrm{d}^2q_{\parallel}}{(2\pi)^4}\int_{-\infty}^{\infty}\mathrm{d}q_2E_q(x)\times\frac{1}{A_0(q)+A_{\parallel}(q)\mathrm{i}\gamma\cdot q_{\parallel}+A_{\perp}(q)\mathrm{i}\gamma\cdot q_{\perp}}\bar{E}_q(y),\quad(8)$$

with scalar and vector quark dressing functions A_0, $A_{\parallel}$, and $A_{\perp}$.

To evaluate Eq. (7), we must know $D_{\mu\nu}(x,y)$. The isotropic Fourier representation of the Landau gauge gluon is given by

$$D_{\mu\nu}(x,y)=\int\frac{\mathrm{d}^4k}{(2\pi)^4}\mathrm{e}^{\mathrm{i}k(x-y)}D(k^2)P_{\mu\nu},\quad(9)$$

where $D(k^2)$ is the gluon propagator function, and $P_{\mu\nu}=\delta_{\mu\nu}-k_\mu k_\nu/k^2$ is the transverse projector. By substituting Eq. (8) and Eq. (9) into Eq. (7), one obtains

$$\Sigma(p,p')=g^2C_F\sum_{L=0}^{\infty}\int\frac{\mathrm{d}^2q_{\parallel}}{(2\pi)^4}\int_{-\infty}^{\infty}\mathrm{d}q_2\int\frac{\mathrm{d}^4k}{(2\pi)^4}\int\mathrm{d}^4x\mathrm{d}^4y\times\bar{E}_p(x)\gamma^{\mu}E_q(x)\frac{1}{A_0(q)+A_{\parallel}(q)\mathrm{i}\gamma\cdot q_{\parallel}+A_{\perp}(q)\mathrm{i}\gamma\cdot q_{\perp}}\times\bar{E}_q(y)\Gamma^{\nu}E_{p'}(y)\mathrm{e}^{\mathrm{i}k(x-y)}D(k^2)P_{\mu\nu},\quad(10)$$

where Γ^{ν} is the dressed quark-gluon vertex, which is unknown in detail, even in the case of vanishing background fields. To make the equations tractable, we resort to a simple ansatz of the form $\Gamma^{\nu}\to\gamma^{\nu}\Gamma(k^2)$, where $\Gamma(k^2)$ is considered independent of the magnetic field.

After some calculations, we can obtain the dressing functions, which are given by [36]

$$A_0(p)|_{L_p=L}=Z_2m_f+C_1\int_q\left\{\left(\frac{A_0(q)}{A_0^2(q)+A_{\parallel}^2(q)q_{\parallel}^2+A_{\perp}^2(q)q_{\perp}^2}\right)\Bigg|_{L_q=L}\cdot\mathrm{e}^{-\frac{k_{\perp}^2}{|2eB|}}G_1(k^2)D(k^2)\Gamma(k^2)\right\}+\frac{C_2}{p_{\parallel}^2}\frac{2}{\tau(L)}\sum_{L_q=L\pm1}\int_q\left\{\left(\frac{A_0(q)}{A_0^2(q)+A_{\parallel}^2(q)q_{\parallel}^2+A_{\perp}^2(q)q_{\perp}^2}\right)\Bigg|_{L_q}\cdot\mathrm{e}^{-\frac{k_{\perp}^2}{|2eB|}}G_2(k^2)D(k^2)\Gamma(k^2)\right\},\quad(11)$$

$$A_{\parallel}(p)|_{L_p=L}=Z_2-\frac{C_1}{p_{\parallel}^2}\int_q\left\{\left(\frac{A_{\parallel}(q)}{A_0^2(q)+A_{\parallel}^2(q)q_{\parallel}^2+A_{\perp}^2(q)q_{\perp}^2}\right)\Bigg|_{L_q=L}\cdot\mathrm{e}^{-\frac{k_{\perp}^2}{|2eB|}}G_3(p,q,k^2)D(k^2)\Gamma(k^2)\right\}+\frac{C_2}{p_{\parallel}^2}\frac{2}{\tau(L)}\sum_{L_q=L\pm1}\int_q\left\{\left(\frac{A_{\parallel}(q)}{A_0^2(q)+A_{\parallel}^2(q)q_{\parallel}^2+A_{\perp}^2(q)q_{\perp}^2}\right)\Bigg|_{L_q}\cdot\mathrm{e}^{-\frac{k_{\perp}^2}{|2eB|}}G_4(p,q,k^2)D(k^2)\Gamma(k^2)\right\},\quad(12)$$

$$A_{\perp}(p)|_{L_p=L}=Z_2+\frac{C_1}{p_{\parallel}^2}\int_q\left\{\left(\frac{A_{\perp}(q)}{A_0^2(q)+A_{\parallel}^2(q)q_{\parallel}^2+A_{\perp}^2(q)q_{\perp}^2}\right)\Bigg|_{L_q=L}\cdot\mathrm{e}^{-\frac{k_{\perp}^2}{|2eB|}}G_5(p,q,k^2)D(k^2)\Gamma(k^2)\right\}-\frac{C_2}{p_{\parallel}^2}\frac{2}{\tau(L)}\sum_{L_q=L\pm1}\int_q\left\{\left(\frac{A_{\perp}(q)}{A_0^2(q)+A_{\parallel}^2(q)q_{\parallel}^2+A_{\perp}^2(q)q_{\perp}^2}\right)\Bigg|_{L_q}\cdot\mathrm{e}^{-\frac{k_{\perp}^2}{|2eB|}}G_6(p,q,k^2)D(k^2)\Gamma(k^2)\right\},\quad(13)$$

where

$$\begin{cases}\tau(L)=2, & L=0,\\ \tau(L)=4, & L>0.\end{cases}\quad(14)$$

We make the following identifications in Eqs. (11)−(13):

$$\int_q=\int\frac{\mathrm{d}^2q_{\parallel}}{(2\pi)^4}\int_{-\infty}^{\infty}\mathrm{d}q_2\mathrm{d}k_1,$$

$$C_1=Z_{1f}g^2C_F,\quad C_2=g^2C_F,$$

$$G_1(k^2)=2-\frac{k_{\parallel}^2}{k^2},\quad G_2(k^2)=2-\frac{k_{\perp}^2}{k^2},$$

$$G_3(p,q,k^2)=p_{\parallel}q_{\parallel}\cos(\varphi)\frac{k_{\parallel}^2}{k^2}-\frac{2[p_{\parallel}q_{\parallel}\cos(\varphi)-p_{\parallel}^2][q_{\parallel}^2-p_{\parallel}q_{\parallel}\cos(\varphi)]}{k^2},$$

$$G_4(p,q,k^2)=\left(2-\frac{k_{\perp}^2}{k^2}\right)p_{\parallel}q_{\parallel}\cos(\varphi),$$

$$G_5(p,q,k^2) = \left(2 - \frac{k_\parallel^2}{k^2}\right) p_\perp q_\perp,$$
$$G_6(p,q,k^2) = \left(\frac{k_1^2 - k_2^2}{k^2}\right) p_\perp q_\perp,$$
$$\cos(\varphi) = \frac{\boldsymbol{p}_\parallel \boldsymbol{q}_\parallel}{|p_\parallel||q_\parallel|}.$$

As we know, solving DSEs in a strong magnetic field is quite difficult. For simplicity, we choose the following forms for the quenched gluon propagator $D(k^2)$ and the vertex dressing function $\Gamma(k^2)$ [36]:

$$D(k^2) = \frac{1}{k^2}\frac{k^2\Lambda^2}{(k^2+\Lambda^2)^2}\left\{\left(\frac{c}{k^2+a\Lambda^2}\right)^b + \frac{k^2}{\Lambda^2}\left[\frac{\beta\alpha(\mu)\log[\frac{k^2}{\Lambda^2}+1]}{4\pi}\right]^\gamma\right\}, \tag{15}$$

$$\Gamma(k^2) = \frac{d_1}{d_2+k^2} + \frac{k^2}{k^2+\Lambda^2}\left[\frac{\beta\alpha(\mu)\log[\frac{k^2}{\Lambda^2}+1]}{4\pi}\right]^{2\delta}. \tag{16}$$

Here, k is the gluon momentum, and the parameters are $a = 0.60$, $b = 1.36$, $\Lambda = 1.4$ GeV, $c = 11.5$ GeV^2, $\beta = 22/3$, $\gamma = -13/22$, $d_1 = 7.9$ GeV^2, $d_2 = 0.5$ GeV^2, $\delta = -18/88$, and $\alpha(\mu) = 0.3$. The quark mass renormalization factor, Z_2, is determined in the renormalization process. The renormalization factor of the quark-gluon vertex is denoted by Z_{1f} and satisfies an approximate Slavnov-Taylor identity in the infrared, as well as the correct ultraviolet running from resummed perturbation theory.

Substituting Eqs. (15)−(16) into Eqs. (11)−(13), one can solve the equations numerically and obtain the quark dressing functions A_0, $A_\parallel$, and $A_\perp$. Note that only A_0 and $A_\parallel$ contribute to the lowest Landau level.

B. Finite volume effects: inclusion of MRE

Eqs. (11)−(13) describe systems in infinite volume. It is meaningful to generalize the previous results to systems of finite volume since quark matter created in RHIC exists in finite size, rather than in the thermodynamic limit. In the present work, we consider the finite volume effects in DSEs using the MRE formalism. The MRE framework, which describes a sphere rather than a cube, is incorporated into the modification of the density of states. This formalism has been applied to calculate the thermodynamic properties of finite-volume quark droplets, successfully reproducing the results obtained from mode-filling calculations [23].

In the MRE formalism, the modified density of states of a finite spherical droplet is written as $q^2\rho_{\rm MRE}/(2\pi^2)$, where $\rho_{\rm MRE}$ is given by [22−25].

$$\rho_{\rm MRE}(q,m_f,R) = 1 + \frac{6\pi^2}{qR}f_{S,f}(q,m_f) + \frac{12\pi^2}{(qR)^2}f_{C,f}(q,m_f)\cdots. \tag{17}$$

Here, m_f is the mass of the quarks, and R is the radius of the sphere. The higher-order terms in $1/R$ correspond to the ellipsis, which are simply neglected here. The function $f_{S,f}(q,m_f)$ corresponding to the surface contribution is given by

$$f_{S,f}(q,m_f) = -\frac{1}{8\pi}\left(1 - \frac{2}{\pi}\arctan\frac{q}{m_f}\right). \tag{18}$$

The function $f_{C,f}(q,m_f)$ corresponding to the curvature contribution is given by

$$f_{C,f}(q,m_f) = \frac{1}{12\pi^2}\left[1 - \frac{3q}{2m_f}\left(\frac{\pi}{2} - \arctan\frac{q}{m_f}\right)\right]. \tag{19}$$

When finite volume effects are considered, the integrals of Eqs. (11)−(13) are replaced by:

$$\int_0^\infty \frac{{\rm d}^3q}{(2\pi)^3}\cdots \to \int_{\Lambda_{IR}}^\infty \frac{{\rm d}^3q}{(2\pi)^3}\rho_{\rm MRE}\cdots. \tag{20}$$

Note that $f_{S,f}(q,m_f)$ and $f_{C,f}(q,m_f)$ have the following massless limits:

$$\lim_{m\to 0} f_{S,f}(q,m_f) = 0, \qquad \lim_{m\to 0} f_{C,f}(q,m_f) = \frac{-1}{24\pi^2}. \tag{21}$$

When $m_f \neq 0$, the MRE density of states can become negative, leading to unphysical results. To eliminate these unphysical values, we introduce an infrared cutoff Λ_{IR}, which is the largest solution of the equation $\rho_{\rm MRE}(q, m_f, R) = 0$ with respect to the momentum q. Although the finite volume effect is accounted for, it should not be corrected in the vertex function at $T = 0$ and $\mu = 0$. The volume effect is a thermodynamic effect that shares the same basis as temperature and chemical potential [37]. When $m_f = 0$, the MRE density of states is given by [25].

$$\rho_{\rm MRE}(q,m_f,R) = 1 - \frac{1}{2(qR)^2}. \tag{22}$$

From Eqs. (20), as well as Eqs. (11)−(13), it is evident that the introduction of the momentum truncation MRE mechanism inevitably imposes constraints on the dressing functions (DF). Consequently, the physical quantities upon which the DF depend are also subject to

such constraints under the MRE mechanism. For instance, when the magnetic field is aligned parallel to the momentum $P_{\parallel}$, it becomes confined within a limited momentum space under this mechanism. These constraints are precisely consistent with the requirements of the thermodynamic limit.

C. The magnetic-field-dependent running coupling constant

As is known, the magnetic field influences the running coupling constant. The coupling constant g in Eqs. (11)−(13) controls the strength of the strong interaction in QCD. Therefore, the magnetic-field (eB)-dependent running coupling constant will have a significant influence on the phase transition of QCD. In the framework of DSEs, the coupling constant g should, in principle, be determined self-consistently, combined with the equations of the quark propagator. However, such a fully self-consistent treatment in the presence of a strong magnetic field is technically challenging and beyond the scope of the present work. Instead, we adopt a phenomenological ansatz for the (eB)-dependent running coupling constant, which has been shown to capture the main features of the magnetic field effect on the QCD coupling in previous studies [30, 38].

In this work, we adopt the eB-dependent running coupling constant [30]

$$g_{\rm II} = \frac{g_{\rm I}}{1 + D_1 \ln\left(1 + D_2 \dfrac{eB}{\Lambda^2_{\rm QCD}}\right)}, \tag{23}$$

where $\Lambda^2_{\rm QCD}$=200 MeV^2, $g_{\rm I}$ is the coupling constant at $eB = 0$, and the free parameters D_1 and D_2 are fixed to obtain reasonable results for the lattice average $(\Sigma_u + \Sigma_d)/2$ [38]. This ansatz effectively incorporates the magnetic field dependence of the coupling while keeping the numerical computation tractable. We note that the consistency with the quark propagator treatment is ensured by the fact that the same coupling constant g enters both the gluon propagator and the quark-gluon vertex in the DSE, and the subtracted quark condensates are in good agreement with lattice QCD data. In our work [34], the subtracted quark condensate is given by

$$\frac{(\Sigma_u + \Sigma_d)}{2} = 1 - \frac{a_1}{eB}\frac{m_L}{m_\pi^2 f_\pi^2}\Big\{[\langle\bar{u}u\rangle_{eB} - \langle\bar{u}u\rangle_{eB=0}] + \big[\langle\bar{d}d\rangle_{eB} - \langle\bar{d}d\rangle_{eB=0}\big]\Big\}, \tag{24}$$

where $m_L = 6$ MeV, $m_\pi = 138$ MeV, $f_\pi = 92.4$ MeV, and $a_1 = 0.04$. The a_1/eB parameter represents the anomalous magnetic moment factor of the external magnetic-dependent chiral condensate, which is compared with the AMM effect (denoted as κ_u, κ_d) in NJL [39].

By applying the expansion in terms of Ritus eigenfunctions, the local quark condensates $\langle\bar{u}u\rangle$ and $\langle\bar{d}d\rangle$ in Eq. (24) can be derived for the case with a magnetic field and are given by

$$-\langle\bar{q}q\rangle = Z_2 N_c \frac{eB}{2\pi^2}\sum_{L_q=0}^{\infty}\frac{\tau(L_q)}{2}\int_0^\infty {\rm d}q_{\parallel}q_{\parallel} \times\left[\frac{A_0(q)}{A_0^2(q) + A_{\parallel}^2(q)q_{\parallel}^2 + A_{\perp}^2(q)q_{\perp}^2}\right]\Bigg|_{L_q}, \tag{25}$$

where $\tau(L_q)$ is given by Eq. (14).

III. NUMERICAL RESULTS

In this section, we present the numerical results for dynamically generated quark condensate, quark mass, and magnetization phenomena, focusing on finite volume effects and magnetic fields. We use the current quark masses, $m_u = 6$ MeV, $m_d = 10$ MeV, and $m_s = 199$ MeV, in simulations. Throughout this paper, our results and analyses are considered at zero temperature ($T = 0$).

Using the solution of the quark's DSEs in strong magnetic fields at zero temperatures, A_0, $A_{\parallel}$, and $A_{\perp}$, we obtain the magnetic dependence of the subtracted quark condensate $(\Sigma_u + \Sigma_d)/2$. Figure 1 shows the magnetic dependence of the subtracted quark condensate $(\Sigma_u + \Sigma_d)/2$, comparing our simulations with the NJL [with AMM ($\bar{\nu} = 0.9$ GeV^{-3}) and without AMM ($\bar{\nu} = 0$ GeV^{-3})] results [39], and the lattice QCD results [38]. We achieve a good fit of the lattice QCD results [38] with $D_1 = 1.50$ and $D_2 = 0.072515$ in Eq. (23).

In the $g_{\rm I}$ case, the subtracted quark condensate increases monotonically with the magnetic field using DSEs, which is indicative of the magnetic catalysis (MC) effect. However, including the eB-dependent running coupling constant (in the $g_{\rm II}$ case) leads to a suppression of the magnetic enhancement effect. This phenomenon originates from: (1) The magnetic-field dependence of the effective coupling manifests as a monotonic decrease with increasing magnetic field (B). This diminishing coupling counteracts the naive magnetic enhancement expected in conventional scenarios. (2) The magnetic field indirectly influences gluon dynamics through its coupling to sea quarks, generating an effect analogous to asymptotic freedom in QCD. This back reaction of gluons constitutes the primary physical origin of the observed suppression. The interplay between these competing mechanisms provides a consistent explanation for the suppression.

Using the solutions of the quark's DSEs, we obtain the constituent quark mass $M = A_0/\sqrt{A_{\parallel}^2 + A_{\perp}^2}$. In Fig. 2, the constituent quark mass M is presented as a function of

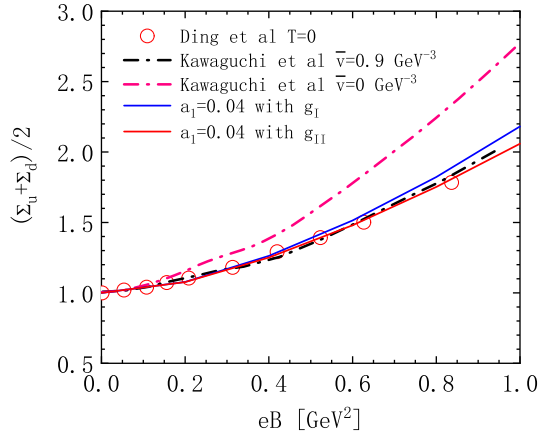

Fig. 1. (color online) The magnetic dependence of the subtracted quark condensate is compared using results from DSEs, the NJL model [39], and lattice QCD data [38].

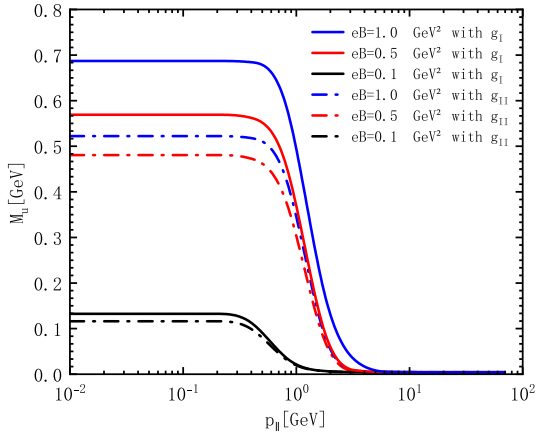

Fig. 2. (color online) Comparison between g_I and g_{II}: constituent quark mass M_u as a function of the momentum $p_\parallel$ for $m_u = 6$ MeV at $eB = 0.1,\ 0.5,\ 1.0$ GeV^2.

the momentum $p_\parallel^2$ at different magnetic fields, $eB = 0.1$, 0.5, 1.0 GeV^2, for the g_I and g_{II} cases, respectively. We find that the constituent quark mass M significantly depends on the running coupling constant. As the magnetic field becomes stronger, the constituent quark mass obviously increases, indicative of magnetic catalysis, as shown in the g_I case. Considering the g_{II} case, in the small momentum region, the mass of the constituent quark M_u drops from 687 to 522 MeV, decreasing by 24% compared to the g_I case at $eB = 1.0$ GeV^2. As the magnetic field becomes stronger, the constituent quark mass drops even more. In the following study, we will concentrate on the finite volume effects in the g_{II} case.

To demonstrate the finite volume effect, we use the MRE formalism and then solve the DSEs in the presence of magnetic fields with the same parameters. Fig. 3(a) and (b) is a supplement to Fig. 2. We display the momentum and finite volume dependence of the constituent quark mass for $m_u = 6$ MeV and $m_s = 199$ MeV based on g_{II} at the magnetic field $eB = 0.5$ GeV^2. We find the masses of constituent quark u show strong volume dependence besides magnetic dependence. In the small momentum region, M decreases obviously with the decrease in radius R, where the finite volume effects become prominent. When the radius decreases from infinity to 2 fm, the mass of the u quark drops from 480 MeV to 310 MeV, and the s quark drops from 597 MeV to 428 MeV. In the large momentum region, M decreases slightly with the decrease of radius R. When the radius R is quite small, the constituent quark mass is small enough to approach the chiral limit. This indicates that the Dynamical Chiral Symmetry Breaking (DCSB) effects reduce with decreasing volumes. The behavior of M approaches that of infinite volume as the radius is large, such as $R \geq 10$ fm, where the finite volume effect can be safely ignored. Our calculations indicate that the DCSB mechanism is realized in idealized systems where the fireball volume is sufficiently large. A similar conclusion has been addressed in prior studies involving DSEs [20]. For a finite volume V, if the condition $V \cdot m \cdot \langle\bar{\Psi}\Psi\rangle \gg \pi$ is satisfied,

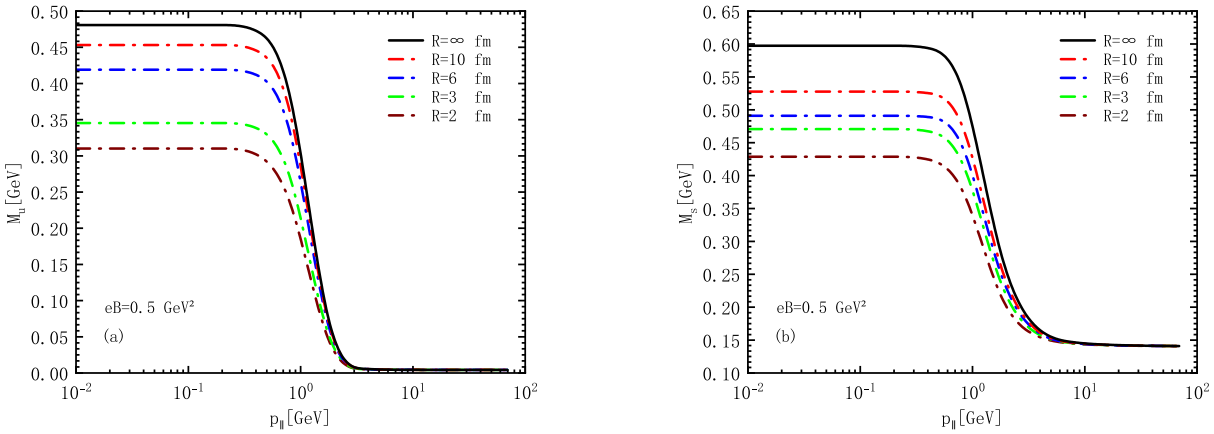

Fig. 3. (color online) Constituent quark mass M_u as a function of the momentum $p_\parallel$ for $m_u = 6$ MeV in (a) and for $m_s = 199$ MeV in (b) for different radii R.

one can still observe the spontaneous formation of quark condensate and the generation of dynamical mass. While within the framework of DSEs, thermodynamic quantities are expected to diverge when $R > 5$ fm [19]. This divergence arises due to the associated length scale of the system becoming physically invalid under such conditions. It should be noted that the radius R dependence arises directly from the MRE approximation employed in this work. A key point of clarification is that the parameter R constitutes a scale variable and does not correspond to a physical coordinate in real space.

To examine the finite volume effects impacting the constituent quark mass, we calculate the partial derivative of M with respect to radius R, $\partial M/\partial R$, for $m_u = 6$ MeV at $eB = 0.1$, 0.5, 1.0 GeV^2, which shows how the range of radius affects M. From Fig. 4, we can see the constituent quark mass M varies with the radius R, and M varies more sharply at stronger magnetic fields. Once again, when $R > 5$ fm, the thermodynamic quantities of the system become invalid [19], leading to an almost zero gradient of mass outside the larger volume. The location of the protrusion in Fig. 4 indicates a sharp variation in the constituent quark mass M for most cases when the radius is confined within a narrow range, approximately between 2 and 6 fm. The narrow range can be increased by the magnetic field, meaning that the strong magnetic field can enhance the finite volume effect.

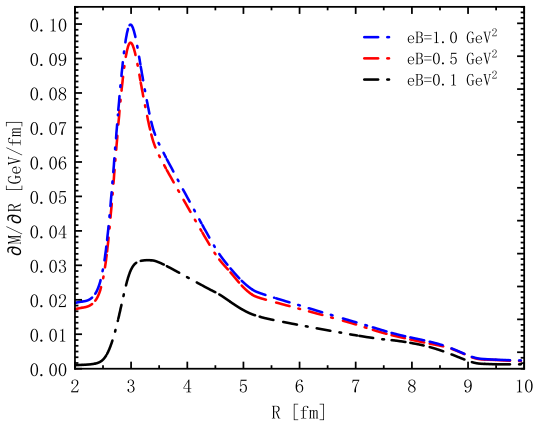

Fig. 4. (color online) The partial derivative with respect to the radius, $\partial M/\partial R$, for $m_u = 6$ MeV at $eB = 0.1$, 0.5, 1.0 GeV^2.

IV. SUMMARY

In summary, we study the finite volume effects of the constituent quark mass in a strong magnetic field based on the framework of DSEs. Since a sufficiently strong magnetic field will affect the running coupling constant, so the coupling constant in DSEs is replaced by the eB-dependent running coupling constant ($g_{\rm II}$) in calculation. In addition, within the MRE formalism, the finite volume effects are considered. The results showed that the constituent quark mass are dependent on the size of fireball besides the magnitude of magnetic field.

(I) With the solutions of the quark's DSEs, we obtain the constituent quark mass M by the quenched ladder approximation in $g_{\rm II}$ case. We also find that in addition to magnetic dependence, the constituent quark mass exhibits a strong running coupling constant dependence. As the magnetic field becomes stronger, M is obviously increased indicative for magnetic catalysis in $g_{\rm I}$ case. While the magnetic enhancement is suppressed, and shows the inverse magnetic catalysis in $g_{\rm II}$ case. In the small momentum region, the masses of constituent quark M_u in the $g_{\rm II}$ case is suppressed 24% more than that in $g_{\rm I}$ case at $eB = 1.0$ GeV^2, *i.g.*, the value of M_u is 687 MeV in $g_{\rm I}$ case and dropped to 522 MeV in $g_{\rm II}$ case. As the magnetic field gets stronger, the constituent quark mass drops even more.

(II) Based on the constituent quark mass in the $g_{\rm II}$ case, we use the MRE formalism to consider the finite volume effects. We calculate the numerical results for the radius of fireball from 2 to 10 fm. The calculation results show that when the momentum is small, M decreases obviously with the decrease of radius R, where the finite volume effects perform prominently. When the momentum is big, M decreases slightly with the decrease of radius R. The behavior of M approaches that of infinite volume as the radius is large, such as $R \geq 10$ fm, where the finite volume effect can safely be ignored. To find out the finite volume effect which affect the constituent quark mass, we calculate the partial derivative of M with respect to radius R. we can observe that the constituent quark mass varies more sharply within a narrow range, approximately between 2 fm and 6 fm.

(III) What we shall pay attention to here is that the MRE formalism is valid only when the system is not sufficiently small size, since the MRE density of states would become negative for too small R. As previously noted, the MRE mechanism exerts a constraining influence on the magnetic field. In this work, however, the external magnetic field is introduced as an input parameter within the DSEs framework. Whether $g_{\rm II}$ should be further modified in a finite volume remains an open question. Given that MRE corrections mainly affect the infrared region while the coupling constant is determined by asymptotic freedom in the ultraviolet, we expect any MRE-induced modifications to $g_{\rm II}$ to be higher-order effects. A detailed quantitative analysis of whether $g_{\rm II}$ should be modified by finite-volume effects will be the focus of future work. In summary, our calculation already shows that the finite volume effects and the magnetic-field-dependent running coupling constant have considerable influence on the phase transition.

References

[1] P. Braun-Munzinger and J. Wambach, Rev. Mod. Phys. **81**, 1031 (2009), arXiv: 0801.4256[hep-ph]
[2] O. Philipsen, Prog. Part. Nucl. Phys. **70**, 55 (2013), arXiv: 1207.5999[hep-lat]
[3] S. Gupta, X. Luo, B. Mohanty *et al.*, Science **332**, 1525 (2011), arXiv: 1105.3934[hep-ph]
[4] M. A. Stephanov, K. Rajagopal, and E. V. Shuryak, Phys. Rev. D **60**, 114028 (1999), arXiv: hep-ph/9903292
[5] M. A. Stephanov, J. Phys. G **38**, 124147 (2011)
[6] A. Bhattacharyya, P. Deb, S. K. Ghosh *et al.*, Phys. Rev. D **87**, 054009 (2013), arXiv: 1212.5893[hep-ph]
[7] P. Braun-Munzinger and J. Stachel, Nature **448**, 302 (2007)
[8] L. F. Palhares, E. S. Fraga, and T. Kodama, J. Phys. G **38**, 085101 (2011), arXiv: 0904.4830[nucl-th]
[9] J. Adams *et al.* (STAR Collaboration), Nucl. Phys. A **757**, 102 (2005), arXiv: nucl-ex/0501009
[10] A. Bhattacharyya, R. Ray, S. Samanta *et al.*, Phys. Rev. C **91**, 041901 (2015), arXiv: 1502.00889[hep-ph]
[11] H. Kohyama, D. Kimura, and T. Inagaki, Nucl. Phys. B **906**, 524 (2016), arXiv: 1601.02411[hep-ph]
[12] J. Braun, B. Klein, and H. J. Pirner, Phys. Rev. D **71**, 014032 (2005), arXiv: hep-ph/0408116
[13] J. Braun, B. Klein, H. J. Pirner *et al.*, Phys. Rev. D **73**, 074010 (2006), arXiv: hep-ph/0512274
[14] H. T. Elze and W. Greiner, Phys. Lett. B **179**, 385 (1986)
[15] S. Samanta, S. Ghosh, and B. Mohanty, J. Phys. G **45**, 075101 (2018), arXiv: 1706.07709[hep-ph]
[16] L. M. Abreu and E. S. Nery, Phys. Rev. C **96**, 055204 (2017), arXiv: 1711.07934[nucl-th]
[17] C. S. Fischer, R. Alkofer, and H. Reinhardt, Phys. Rev. D **65**, 094008 (2002), arXiv: hep-ph/0202195
[18] B. L. Li, Z. F. Cui, B. W. Zhou *et al.*, Nucl. Phys. B **938**, 298 (2019), arXiv: 1711.04914[hep-ph]
[19] Y. Z. Xu, C. Shi, X. T. He *et al.*, Phys. Rev. D **102**, 114011 (2020), arXiv: 2009.12035[nucl-th]
[20] J. Bernhardt, C. S. Fischer, P. Isserstedt *et al.*, Phys. Rev. D **104**, 074035 (2021), arXiv: 2107.05504[hep-ph]
[21] L. Jiang, F. Gao, and Y. x. Liu, Eur. Phys. J. C **85**, 807 (2025), arXiv: 2310.15770[nucl-th]
[22] R. Balian and C. Bloch, Annals Phys. **60**, 401 (1970)
[23] J. Madsen, Phys. Rev. D **50**, 3328 (1994), arXiv: hep-ph/9407314
[24] O. Kiriyama and A. Hosaka, Phys. Rev. D **67**, 085010 (2003), arXiv: hep-ph/0211235
[25] O. Kiriyama, Phys. Rev. D **72**, 054009 (2005), arXiv: hep-ph/0507188
[26] N. Chahal, S. Dutt, and A. Kumar, Phys. Rev. C **107**, 045203 (2023), arXiv: 2303.16840[hep-ph]
[27] P. Adhikari and B. C. Tiburzi, Phys. Rev. D **107**, 094504 (2023), arXiv: 2302.09179[hep-lat]
[28] A. Ayala, S. Bernal-Langarica, and C. Villavicencio, Phys. Rev. D **105**, 056001 (2022), arXiv: 2111.05951[hep-ph]
[29] V. A. Miransky and I. A. Shovkovy, Phys. Rev. D **66**, 045006 (2002), arXiv: hep-ph/0205348
[30] R. L. S. Farias, K. P. Gomes, G. I. Krein *et al.*, Phys. Rev. C **90**, 025203 (2014), arXiv: 1404.3931[hep-ph]
[31] E. J. Ferrer, V. de la Incera, and X. J. Wen, Phys. Rev. D **91**, 054006 (2015), arXiv: 1407.3503[nucl-th]
[32] R. L. S. Farias, V. S. Timoteo, S. S. Avancini *et al.*, Eur. Phys. J. A **53**, 101 (2017), arXiv: 1603.03847[hep-ph]
[33] W. R. Tavares, R. L. S. Farias, S. S. Avancini *et al.*, Eur. Phys. J. A **57**, 278 (2021), arXiv: 2104.11117[hep-ph]
[34] D. X. Wei and L. J. Zhou, Int. J. Mod. Phys. E **32**, 2350024 (2023), arXiv: 2212.03508[hep-ph]
[35] L. J. Zhou, B. Zheng, H. W. Zhong *et al.*, Chin. Phys. C **39**, 033101 (2015), arXiv: 1403.6965[hep-ph]
[36] N. Mueller, J. A. Bonnet, and C. S. Fischer, Phys. Rev. D **89**, 094023 (2014), arXiv: 1401.1647[hep-ph]
[37] A. Sarkar, P. Deb, B. Mandal *et al.*, (2025), arXiv: 2507.21744 [hep-ph]
[38] H. T. Ding, S. T. Li, J. H. Liu *et al.*, Phys. Rev. D **105**, 034514 (2022), arXiv: 2201.02349[hep-lat]
[39] M. Kawaguchi and M. Huang, Chin. Phys. C **47**, 064103 (2023), arXiv: 2205.08169[hep-ph]